JOC The Journal of Organic Chemistry

Article

pubs.acs.org/joc

Reductive Ring Closure Methodology toward Heteroacenes Bearing a Dihydropyrrolo[3,2-*b*]pyrrole Core: Scope and Limitation

Li Qiu,[†,§] Xiao Wang,[†] Na Zhao,[†,§] Shiliang Xu,[†,‡] Zengjian An,[†] Xuhui Zhuang,[†,§] Zhenggang Lan,[†] Lirong Wen,[‡] and Xiaobo Wan*[,†]

[†]CAS Key Laboratory of Biobased Materials, Qingdao Institute of Bioenergy & Bioprocess Technology, Chinese Academy of Sciences, Qingdao, 266101, People's Republic of China

[‡]State Key Laboratory Base of Eco-Chemical Engineering, College of Chemistry and Molecular Engineering, Qingdao University of Science and Technology, Qingdao 266042, People's Republic of China

[§]University of Chinese Academy of Sciences, Beijing 100049, People's Republic of China

Supporting Information

ABSTRACT: A newly developed reductive ring closure methodology to heteroacenes bearing a dihydropyrrolo[3,2-*b*]pyrrole core was systematically studied for its scope and limitation. The methodology involves (i) the cyclization of an *o*-aminobenzoic acid ester derivative to give an eight-membered cyclic dilactam, and (ii) the conversion of the dilactams into the corresponding diimidoyl chloride, which undergoes (iii) reductive ring closure to install the dihydropyrrolo[3,2-*b*]pyrrole core. The first step of the methodology plays the key role due to its substrate limitation, which suffers from the competition of oligomerization and hydrolysis. All the dilactams could successfully convert to the corresponding diimidoyl chlorides, most of which succeeded to give the dihydropyrrolo[3,2-*b*]pyrrole core. The influence of the substituents and the elongation of conjugated length on the photophysical properties of the obtained heteroacenes were then investigated systematically using UV−vis spectroscopy and cyclic voltammetry. It was found that chlorination and fluorination had quite a different effect on the photophysical properties of the heteroacene, and the ring fusing pattern also had a drastic influence on the band gap of the heteroacene. The successful preparation of a series of heteroacenes bearing a dihydropyrrolo[3,2-*b*]pyrrole core would provide a wide variety of candidates for further fabrication of organic field-effect transistor devices.

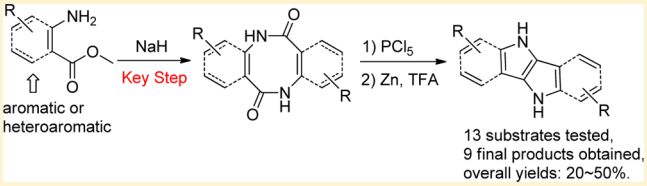

INTRODUCTION

Linear extended π-conjugated acenes with a central heterocycle arouse much attention in recent years due to their potential applications as organic semiconductors.[1,2] For instance, heteroacenes bearing a thieno[3,2-*b*]thiophene core and its seleno analogue were synthesized, and their properties were systematically studied. Organic field-effect transistors (OFETs) based on these materials exhibited high charge carrier mobility up to 31.3 $cm^2 \cdot V^{-1} \cdot s^{-1}$.[3−15] This progress was also accompanied by the discovery of novel routes toward such heteroacenes,[3,5,14,16] which enriched the synthetic methodology of heterocycles.

Our attention was focused on heteroacenes bearing a dihydropyrrolo[3,2-*b*]pyrrole core, which are more electron-rich than thieno[3,2-*b*]thiophene and can be easily alkylated to make them soluble in common organic solvents for solution-processable OFETs. The parent dihydropyrrolo[3,2-*b*]pyrrole is very oxygen-sensitive and is difficult to synthesize due to its strong electron-rich character.[17] On the other hand, its analogue, 5,10-dihydroindolo[3,2-*b*]indole (DHII, Scheme 1, compound **1a**), is chemically stable. Although the first synthesis of DHII was reported more than a century ago, the synthetic routes toward it were quite limited until recently.[18] The first route was based on the reduction of dinitrotolane (Scheme 1, compound **2**) using $SnCl_2$ as the reducing reagent in a mixture of HCl/AcOH at high temperature (Scheme 1, Route 1).[19] Several modifications on this method were reported later.[20] This method was still used recently in the preparation of indolo[3,2-*b*]indole-based conjugated polymers, although expensive noble-metal catalyst was used and the overall yield was low.[21,22] An alternative method was later developed by Kaszynski et al.,[23] in which 2,2′-diaminostilbene **3** was converted into the corresponding azide, which cyclized at 155 °C to give DHII as a side product (Scheme 1, Route 2). Fischer indole synthesis was also applied to indolin-3-one **4** to afford N-protected indolo[3,2-*b*]indole in moderate yield (Scheme 1, Route 3).[24] Heating *o*-nitrophenylindole with $P(OEt)_3$ was also reported to give indolo[3,2-*b*]indole in good yield.[25] However, all these methods suffer from either low yields or limited availability of starting materials, which limits the intensive investigation of the potential applications of indolo[3,2-*b*]indole derivatives. We also noticed that recently a novel method to construct tetraaryl-1,4-dihydropyrrolo[3,2-*b*]pyrrole

Received: June 23, 2014
Published: October 23, 2014

   dx.doi.org/10.1021/jo501402n | J. Org. Chem. 2014, 79, 11339−11348

Scheme 1. Synthetic Routes towards DHII

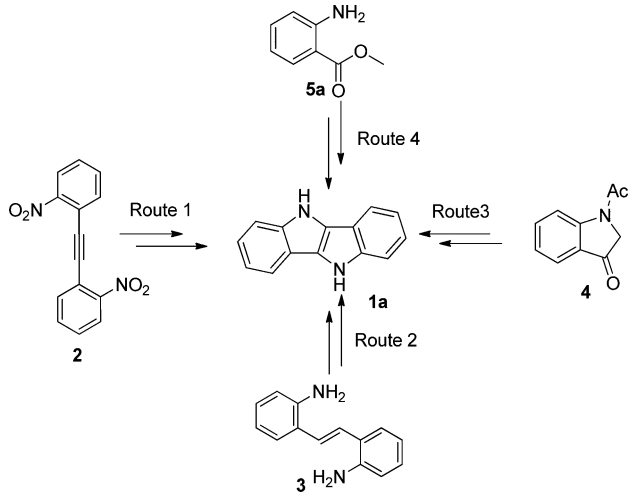

was reported, which will further broaden the research in this area.[26,27]

We recently reported a novel synthetic strategy toward dihydropyrrolo[3,2-*b*]pyrrole derivatives. Starting from easily available *o*-aminobenzoate, DHII was synthesized in three steps in 33% overall yield (Scheme 1, Route 4).[28] By applying the same methodology to 3-amino-2-naphthoate, longer heteroacene bearing a dihydropyrrolo[3,2-*b*]pyrrole core was also synthesized in satisfying yield.[29] The methodology involves (i) the cyclization of an *o*-aminobenzoic acid ester derivative to give eight-membered cyclic dilactams, and (ii) the conversion of the dilactams into the corresponding imidoyl chloride, which undergoes (iii) reductive ring closure to install the dihydropyrrolo[3,2-*b*]pyrrole core. Given the easy accessibility of *o*-aminobenzoic acid ester derivatives, this methodology might pave a broad way toward heteroacenes bearing a dihydropyrrolo[3,2-*b*]pyrrole core and give an opportunity to systematically investigate the influence of the substituents on the properties of such heteroacenes. We herein report a systematic study on the scope and limitation of this methodology and the comparison on the optical and electrochemical properties of the resultant heteroacenes.

RESULTS AND DISCUSSION

Synthesis. *Formation of the Eight-Membered Cyclic Dilactams.* The key reaction in the synthetic route toward heteroacenes bearing a dihydropyrrolo[3,2-*b*]pyrrole core is the cyclization of *o*-aminobenzoate **5a**, which leads to the formation of the corresponding eight-membered cyclic dilactams. This method was first reported by Cooper et al., using powdered sodium in dry benzene as the base.[30] The yield of the cyclic dilactams was later improved by employing NaH as the base.[31,32] However, no systematic study was performed on whether the other substituents on the benzene ring will influence the outcome of this reaction. Although the cyclization of methyl 2-amino-5-methylbenzoate gave similar results, the influence of the methyl group on the electronic character of the phenyl ring was not significant. The influence of strong electron-donating groups or electron-withdrawing groups on the cyclization reaction has not been investigated. On the other hand, whether the cyclization could be expanded to other heterocycles is still a question to be answered. The only example appearing in the literature is the cyclization of methyl 2-aminonicotinate, which resulted in the cyclic dilactams with low yield.[33]

Considering these aspects, a series of aromatic/heteroaromatic compounds bearing adjacent amino and ester groups were either purchased or synthesized to investigate the influence of these two factors. The results are shown in Table 1, column 2. The effect of the expansion of the aromatic ring was first investigated. No difficulties were encountered in cyclizing methyl 3-amino-2-naphthoate (**5b**) or its isomer methyl 1-amino-2-naphthoate (**5c**) (Table 1, entries 2 and 3). However, methyl 10-aminophenanthrene-9-carboxylate (**5d**) could not be cyclized under similar conditions (Table 1, entry 4), and an insoluble material was obtained and speculated to be

Table 1. Scope and Limitation of Reductive Ring Closure Methodology

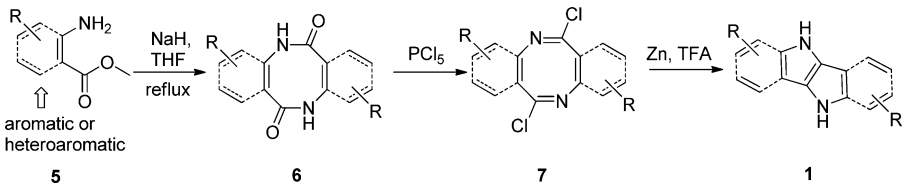

entry	substrates[a]	yield (%) of **6**[b]	yield (%) of **7**	yield of **1**
1	**5a**	75	64	70
2	**5b**	75	60	50
3	**5c**	70		30[d]
4	**5d**	oligomer		
5	**5e**/**5e′**	70	45	
6	**5f**	95		53[d]
7	**5g**	75[c]		35[d]
8	**5h**	60[c]		37[d]
9	**5i**	26[c]		37[d]
10	**5j**	oligomer		
11	**5k**	26		37[d]
12	**5l**	90	45	67
13	**5m**	96	50	

[a]For chemical structures, see Scheme 2. [b]Yield of the crude product which was used directly in the next step. [c]Isolated yield. [d]Yield of two steps.

dx.doi.org/10.1021/jo501402n | J. Org. Chem. 2014, 79, 11339−11348

Scheme 2. Structures of the Substrates 5 Tested

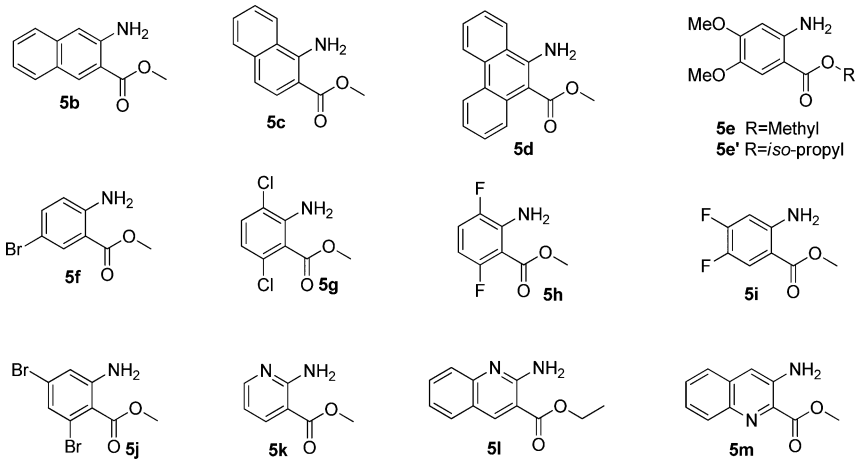

the oligomer of a linear polyamide. Comparing **5d** with **5c**, it might be concluded that fusing one more phenyl ring adjacent to the ester group has a dramatic influence on the reaction.

The substitution on the phenyl ring of *o*-aminobenzoate also has a marked influence on the reaction. Compound **5e**, which is electron-rich due to the presence of two phenol ether groups, failed to give any cyclic dilactam. Instead, the complete hydrolysis of **5e** was observed. We noticed that when NaH was used as the base, hydrolysis of the ester group was also a side reaction in the formation of cyclic dilactams in other cases because NaH is hydroscopic and a trace amount of NaOH was inevitably introduced during its storage. However, even when strict anhydrous conditions were adopted, the complete hydrolysis of **5e** was still observed. It seems that the existence of strong electron-donating groups on the benzene ring promotes the hydrolysis of the methyl benzoate, which overwhelms the cyclization reaction. Based on this hypothesis, a more robust isopropyl ester **5e′** was used; the hydrolysis reaction was suppressed, and cyclic diamide **6e** was then obtained in 75% yield. On the other hand, an electron-withdrawing group does not influence the cyclization that much. Bromination at the *para*-position to the amino group even favored the cyclization, and the cyclic dilactam yield improved to 95% (Table 1, entry 6). Double chloro- and fluoro- substituted methyl aminobenzoate, which are more electron-deficient, could also be cyclized and afforded the corresponding cyclic dilactams with similar yields compared to the unsubstituted one (Table 1, entries 7−10). The exception is **5i**, which only afforded the cyclic dilactams in 26% yield, due to the occurrence of S_NAr substitution as the side reaction. Surprisingly, double bromo-substituted aminobenzoate **5j**, with one of the bromine atom at the *ortho*-position of the ester group, failed to cyclize (Table 1, entry 11). An insoluble oligoamide was obtained, similar to the case of **5d**. It might be attributed to the steric hindrance introduced by the bromine atom, which is much larger in size than chlorine and fluorine atoms.

The possibility to extend the cyclization reaction to heterocycles was also studied. As reported in the literature, the cyclization of methyl 2-aminonicotinate **5k** gave cyclic dilactam in low yield (26%). However, we were delighted to find out that quinoline-based amino acid derivatives produce the corresponding cyclic dilactam in excellent yield (over 90% Table 1, entries 12 and 13). It could be concluded that the proper electron-deficient character of the aromatics with an amino group and an ester group at adjacent positions seems to favor the cyclization reaction, while the electron-rich one does not.

Synthesis of Heteroacenes Bearing a Dihydropyrrolo[3,2-b]pyrrole Core. With 11 cyclic dilactams in hand, we tested their ability to form the final heteroacenes bearing a dihydropyrrolo[3,2-*b*]pyrrole core. In all cases, the formation of the diimidoyl chloride **7** was achieved with no exceptions. As the diimidoyl chloride derivatives are prone to hydrolyze back to the corresponding dilactams under acidic conditions and the unreacted PCl_5 and the byproducts (HCl (gas) and $POCl_3$) from the reaction are all hydroscopic, the crude product needed to be handled with care. After HCl (gas) and $POCl_3$ were evaporated together with the solvent thoroughly, diimidoyl chlorides **7a**,**b**, **7e**, and **7l**,**m** could be purified by quickly passing through a short silica column chromatography. However, not all of the diimidoyl chlorides could survive this purification condition. We then found out that they could be directly used for the next step without further purification, as long as the purity of the corresponding precursors (cyclic dilactams **6**) could be guaranteed. For the reductive ring closure step, nine heteroacenes bearing the dihydropyrrolo[3,2-*b*]-pyrrole core were synthesized, all in similar yield (around 30−50% for two steps). The two exceptions are compounds **7e** and **7m**. A deep-blue colored crude was obtained during the reductive ring closure of compound **7e**, which could not be purified. This might be due to the strong electron-rich nature of compound **1e**, which might undergo further oxidation during purification to give the colored crude. However, no more information about this crude could be obtained at this stage. On the other hand, the failure to synthesize **1m** from **7m** was due to some other reasons: 2-methylquinolin-3-amine was isolated as the fully reduced product. In conclusion, if the eight-membered cyclic dilactams could be synthesized, then in most cases, the subsequent chlorination and reductive ring closure would lead to the desired heteroacenes of the dihydropyrrolo-[3,2-*b*]pyrrole core. The most difficult step is the cyclization step toward the eight-membered cyclic dilactams.

Influence of the Substituents on the Photophysical Properties of the Heteroacenes. In order to have a rough idea about the potential use of heteroacenes bearing a dihydropyrrolo[3,2-*b*]pyrrole core in organic electronics, we explored their photophysical properties in advance, which gave

dx.doi.org/10.1021/jo501402n | J. Org. Chem. 2014, 79, 11339−11348

Scheme 3. Structures of Six C8-Alkylated Heteroacenes Tested for Photophysical Properties

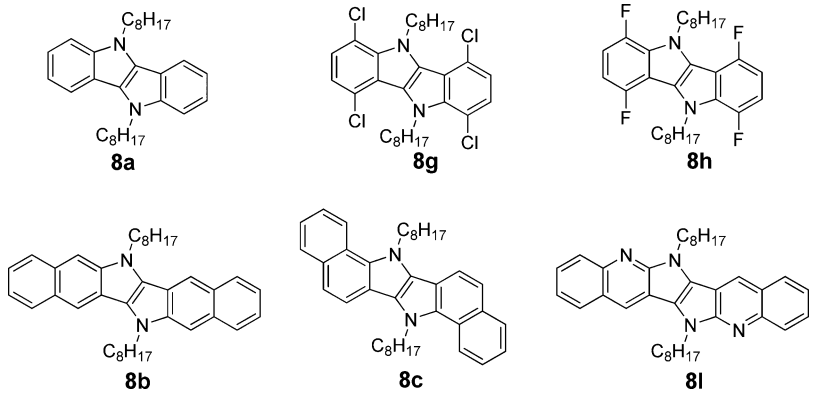

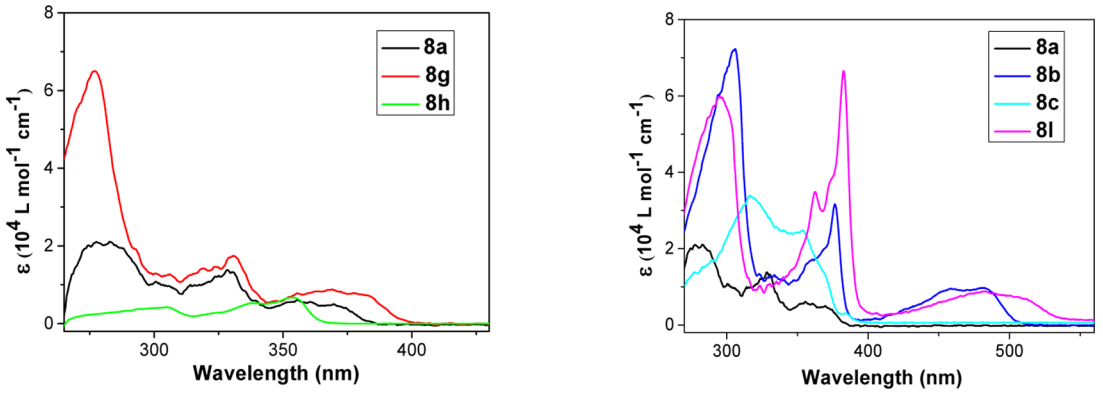

Figure 1. UV−vis absorption of six C8-alkylated heteroacenes in THF (**8a**, **8b**, **8g**, and **8l** were recorded at 10^{-5} mol/L; **8c** was recorded at 2×10^{-5} mol/L; **8h** was recorded at 10^{-4} mol/L).

us the information about their front orbital energy levels, energy gaps, and electrochemical stability. Furthermore, due to the successful synthesis of all the derivatives of the heteroacenes with a dihydropyrrolo[3,2-*b*]pyrrole core, a systematic structure−property relationship of these heteroacenes could be obtained from these photophysical data. Thus, the UV−vis absorption spectra and cyclic voltammetry diagrams of these heteroacenes were recorded and compared. Six selected heteroacenes were alkylated (Scheme 3; synthesis details are shown in the Experimental Section) to improve their solubility in organic solvents so that high-quality UV−vis spectra and electrochemical diagrams could be obtained.

Electronic Absorption Spectroscopy. Six alkylated heteroacenes were divided into two categories. Compounds **8a**, **8g**, and **8h** were grouped to compare the influence of halogenation on the photophysical properties of the heteroacenes, while compounds **8b**, **8c**, and **8l** were grouped to compare the fusion pattern and the introduction of heterocycles on the photophysical properties of the heteroacenes. UV−vis absorption spectra of six C8-alkylated heteroacenes are shown in Figure1. The influence of halogenation was investigated first (**8a**, **8g**, and **8h**). The halogenation has a dramatic influence on the intensity of the absorption bands, as shown by the molar extinction coefficients (ε). Chlorination leads to a stronger absorption ($\varepsilon_{max} \sim 6.5 \times 10^4$ L·mol^{-1}·cm^{-1}), while fluorination leads to a weaker absorption ($\varepsilon_{max} \sim 0.64 \times 10^4$ L·mol^{-1}·cm^{-1}), compared to the parent indolo[3,2-*b*]indole ($\varepsilon_{max} \sim 2.0 \times 10^4$ L·mol^{-1}·cm^{-1}). Since the intensity of absorption is largely dependent on the probability of interaction between the irradiation energy and the electronic system and the transition moment during excitation, it could be concluded that chlorination on the indolo[3,2-*b*]indole core might either induce a larger change in the transition absorption or increase the probability of the interaction between the irradiation energy and the chromophore. Despite the difference in molar absorptivity, the absorption spectra of **8a** and **8g** in THF are similar, which show three main absorption bands. To assign the absorption, theoretical calculations were conducted by the DFT (B3LYP/6-3+G*) method embedded in the Gaussian 09 software package (see Supporting Information). The lowest energy absorption centered at 370 nm is assigned to S0 → S1 band excitation, and the fine structure of the absorption might be due to the near overlap of the vibronic transitions between the molecular electronic ground state S0 and the first excited one S1 in the heteroacene. The absorption around 330 nm with a weak shoulder is assigned to S0 → S2 excitation, and the most intense one at 275 nm is assigned to the higher energy absorption (S0 → S5). The phenomenon reflects that the introduction of Cl substituents on the benzene ring has little effect on the absorption and, hence, the electronic structure of the heteroacene. On the other hand, the F substitutions seem to have a great influence on it, as evidenced by the absorption spectrum of **8h**, which shows that both S0 → S1 and S0 → S2 bands are blue-shifted (one from 370 to 350 nm with better fine structure solution and the other from 330 to 300 nm overlapped with the third band at 275 nm). The obvious blue shift of the absorption edge of fluorinated indolo[3,2-*b*]indole indicates that fluorination has a dramatic influence on the band gap of the heteroacene (S0 → S1 band is assigned to HOMO → LUMO transition according to the calculation). The

dx.doi.org/10.1021/jo501402n | J. Org. Chem. 2014, 79, 11339−11348

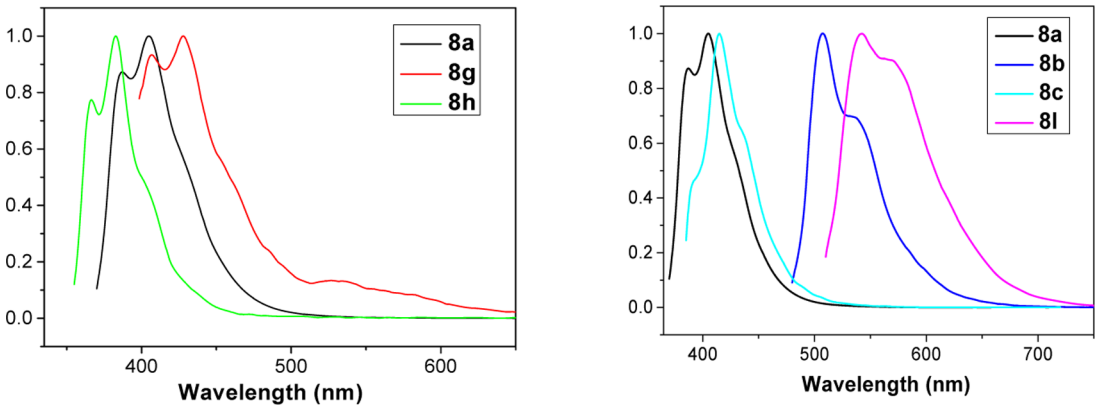

Figure 2. Normalized fluorescence spectra of six C8-alkylated heteroacenes in THF.

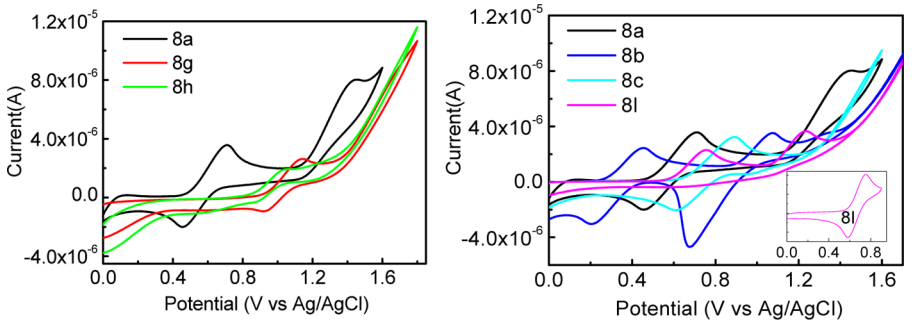

Figure 3. Cyclic voltammetric diagrams of six C8-alkylated heteroacenes in chloroform (electrolyte: Bu_4NPF_6 (0.1 M), scan rate = 0.1 V s^{-1}).

different effects of chlorination versus fluorination might be from their different influence on the frontier orbitals, which is the balance of their inductive withdrawal effects and the lone-pair back-donation effects to the sp^2-C of the backbone. This difference is also commonly seen in other conjugated counterparts with Cl and F substitutions[34] and will be discussed later in detail.

The influence of the extension of the effective conjugated length on the dihydropyrrolo[3,2-*b*]pyrrole core was then investigated (**8a**, **8b**, **8c**, and **8l**). Compound **8b**, which is the π-extended derivative of **8a** with two linearly fused benzene rings, showed a drastic red shift (more than 100 nm) of the absorption edge. On the other hand, compound **8c**, which is the π-extended derivative of **8a** with two angularly fused benzene rings, showed a slightly blue-shifted absorption edge (from 404 to 396 nm), but with the red-shifted S0 → S2 bands (from 275 to 318 nm) and S0 → S5 bands (from 330 to 350 nm). This indicates that the angularly fused benzene rings have little effect on the band gap of the dihydropyrrolo[3,2-*b*]pyrrole core and might be caused by the inefficiency of π-conjugation due to the angular fusion pattern. It also infers that in the design of larger heteroacenes for effective conjugation, the fusing pattern should also be taken into consideration. Furthermore, compound **8l**, which could be considered as the derivative of **8b** with the center benzene ring replaced by a pyridine ring, showed a further red shift of the absorption edge to 542 nm and strongly enhanced S0 → S2 bands. This indicates that replacing a benzene ring with a pyridine ring on the backbone (from **8b** to **8l**) further lowers the band gap. This observation is in agreement with the electron-withdrawing nature of unsaturated N atoms, which was also observed in comparison to TIPs-pentacene and its *N*-hetero analogue.[35] It is also worthwhile to note that the molar extinction coefficients also exhibit a strong correlation with the effective increase of the conjugated length. Compared with **8a**, the linear expansion of the conjugation (**8c** and **8l**) leads to an obvious increase of the ε_{max} value to more than 6.5×10^4 $L \cdot mol^{-1} \cdot cm^{-1}$; however, the angular expansion of the conjugation (**8b**) has much less influence.

The fluorescence spectra of **8a**, **8b**, **8c**, **8g**, **8h**, and **8l** in THF (10^{-5} to 10^{-6} mol/L) are shown in Figure 2, which were excited on their absorption maxima values, respectively. All six compounds are fluorescent with color ranging from violet to yellow, and two well-defined vibronic maxima were observed. Chlorination leads to the red shift, while fluorination leads to the blue shift of the fluorescence emission, which is in accordance with the influence on the UV−vis spectra. On the other hand, the linear expansion of the conjugation (**8c** and **8l**) leads to an obvious red shift of the fluorescence emission, while the angular expansion of the conjugation emission (**8b**) causes little red shift.

Electrochemistry. In order to elucidate the effects of the substitutions and elongation of the conjugated length on the electron-donating character and the electrochemical stability, we investigated the energy levels of the frontier molecular orbitals of six selected alkylated heteroacenes bearing a dihydropyrrolo[3,2-*b*]pyrrole core by performing their cyclic voltammetry (CV) in chloroform (Figure 3). The oxidation potentials ($^{ox}E_{1/2}$) and energy levels are listed in Table 2.

The effect of halogenation was investigated first. As can be seen in Figure 3, the CV of **8a** shows a pair of oxidation waves, with the first being semireversible and the second being irreversible, with two oxidation potentials $^{ox}E_{1/2}$ (0.54 and 1.29 V). Since the electronegative substitution tends to attenuate the electron-donating character by lowering the HOMO's energy level of the resulting molecules, chlorinated **8g** and fluorinated

dx.doi.org/10.1021/jo501402n | J. Org. Chem. 2014, 79, 11339−11348

Table 2. Photophysical Properties of Acenes[a]

compound	λ_{edge} (nm)	E_g (eV)[b]	$^{ox}E_{1,1/2}$ (eV)	$^{ox}E_{2,1/2}$ (eV)	$^{ox}E_{onset}$ (eV)	E_{HOMO} (eV)[c]	E_{LUMO} (eV)[d]
8a	404	3.07	0.54	1.29	0.50	−4.82	−1.75
8g	404	3.07	1.03		0.93	−5.25	−2.18
8h	367	3.38	0.94		0.86	−5.18	−1.80
8b	510	2.43	0.34	0.91	0.29	−4.61	−2.18
8c	396	3.13	0.75		0.65	−4.97	−1.84
8l	542	2.29	0.68	1.1	0.59	−4.91	−2.62

[a]0.001 M in THF, V vs Ag/Ag^+ in 0.1 M Bu_4NPF_6/THF, scan rate = 0.1 V s^{-1}, 25 °C. Ferrocene was used as a standard. [b]Determined from UV−vis absorption spectra. [c]$E_{HOMO} = -(^{ox}E_{onset} + 4.32)$ eV. [d]$E_{LUMO} = (E_{HOMO} + E_g)$ eV.

8h are more difficult to be oxidized, as evidenced by the increase of the first $^{ox}E_{1/2}$ to 1.03 and 0.94 V, respectively. Interestingly, **8g** is even more difficult to be oxidized compared with **8h**, reflecting a better electron-withdrawing effect of the chlorine atom compared with the fluorine atom. At first glance, this result seems to be conflicting with the fact that fluorine is much more electronegative than chlorine. However, it could be explained by the back-donation effect of the electron-donating lone pair on the two halogens. Although the fluorine atom is more electronegative, its 2p nonbonding lone pairs overlap better with the 2p orbital of the sp^2-C due to the similar energy level of the two orbitals of fluorine and carbon, hence its lone pair has a better electron-donating effect toward the benzene ring. On the other hand, the 3p nonbonding lone pairs of chlorine are less effective in resonance donation to the 2p orbital of carbon, due to a much larger difference of energy level between chlorine and carbon compared with the one between fluorine and carbon. Overall, the electron-withdrawing effect of the fluorine atom is largely weakened by the electron-donating effect of its lone pair, while this back-donation effect is much weaker in the chlorine atom. So, chlorine is a better electron-withdrawing group than fluorine in π-conjugated systems. The observation that chlorination generally gives lower HOMO and smaller HOMO−LUMO gap (see Figure 3) than fluorination is also seen in other conjugated systems with Cl and F substituents.[34,36]

The effects of increasing the effective conjugated length via fusing more aromatic rings to the DBII and the effect of incorporation of electron-deficient heterocycles were then investigated. Compound **8b** is the linear π-extension derivative of **8a** and showed a much lower oxidation potential onset at 0.34 V, which is in accordance with the rule that the oxidation potential of π-conjugated systems decreases with the increase of the conjugated length. In sharp contrast, compound **8c**, which is the angular π-extension derivative of **8a**, did not lower the oxidation potential but showed a slight higher oxidation potential onset at 0.65 V than **8a**. This result indicates that the angularly fused benzene ring to **8a** does not increase the effective conjugated length of **8a** and is also consistent with the observation of its UV−vis absorption. Compound **8l**, which is also the linear π-extension derivative of **8a** but with the center benzene rings replaced by pyridine rings, showed an oxidation potential onset at 0.59 V, which is 0.3 V higher than that of **8b** with the same effective conjugated length. This indicates that the incorporation of electron-deficient heteroaromatics effectively lowered the HOMO energy level of the heteroacenes.

The influence of the increase of effective conjugated length and the incorporation of electron-deficient pyridine rings on the reversibility of the electrochemical redox process is also interesting. Compared with **8a**, which only showed one pair of semireversible redox waves, compound **8b** showed two pairs of semireversible redox waves. Compound **8c**, on the other hand, similar to compound **8a**, only showed one pair of semireversible redox waves. These results are in accordance with the fact that **8b** showed effectively increased effective conjugated length but **8c** did not, indicating that the reversibility of such heteroacenes could be improved by linear incorporation of a benzene ring to the center core. Compared to **8b**, compound **8a** only showed a pair of reversible redox waves (the inset in Figure 3) if the voltage was scanned to 0.9 V (vs Ag/AgCl). When further scanned to higher potentials, a second oxidative peak appeared, which is irreversible, and the first redox pair became irreversible, too. This could be explained by the electron-deficient character of the pyridine ring: in the second redox process, a dication is generated, which becomes less stable and undergoes further decomposition because **8l** is more electron-poor than **8b**. For all the alkylated heteroacenes mentioned above, we also tested whether they could be electrochemically reduced. However, no reduction wave was observed in the tested electrochemical window (0 to −2.0 V vs Ag/AgCl), indicating that these heteroacenes are electron-rich and could not be used as n-type semiconductors.

Based on data from UV−vis spectra and CV diagrams (Table 2), the different effects of the substituents and the conjugation length on the frontier orbitals of the heteroacenes bearing a dihydropyrrolo[3,2-*b*]pyrrole core could be visually summarized in Figure 4: (1) Chlorination lowered both the energy

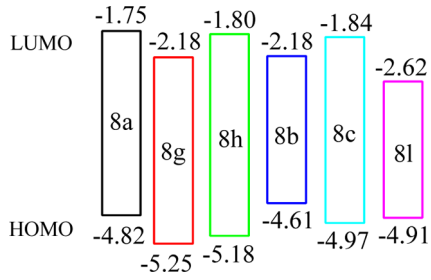

Figure 4. Energy diagrams (eV) of six C8-alkylated heteroacenes.

level of both the HOMO and the LUMO to a similar extent (0.43 eV) due to its electron-withdrawing effect, so it did not lead to a smaller band gap. On the other hand, fluorination lowered the HOMO level by 0.36 eV but had little influence on the LUMO level, so the band gap was enlarged. This results in the different photophysical properties of the corresponding halogenated heteroacenes. (2) Linearly fused benzene rings could effectively raise the HOMO and lower the LUMO levels, while the angularly fused one just lowered both the HOMO and the LUMO levels slightly. This means that, to approach an effective conjugation for larger heteroacenes, a linear fusion pattern would be a better choice than the angular one. (3) Unlike halogenation, the inclusion of a stronger electron-withdrawing sp^2-hybridized N atom could effectively lower both the HOMO and the LUMO levels, and the drop of LUMO is apparently greater than that of HOMO, which would be a preferred way to obtained n-type semiconductors.

CONCLUSION

In summary, we have systematically studied the scope and limitation of our newly developed reductive ring closure

dx.doi.org/10.1021/jo501402n | J. Org. Chem. 2014, 79, 11339−11348

methodology to heteroacenes bearing a dihydropyrrolo[3,2-*b*]pyrrole core and also investigated the influence of the substituents on the photophysical properties of such heteroacenes. The first step of the methodology (the cyclization of the *o*-aminobenzoate derivatives to give the eight-membered dilactam) seems to play the key role due to its substrate limitation. This step suffers from the competition of oligomerization and hydrolysis. To be more precise, the large *ortho*-substituents to the ester group hindered the cyclization and led to the formation of oligomers (in the cases of **5d** and **5j**), and an electron-donating group on the phenyl ring promoted hydrolysis (in the case of **5e**). The hydrolysis could be effectively suppressed by using a more robust isopropyl ester instead of the methyl ester, and then the cyclization would be favored (in the case of **5e′**). On the other hand, the electron-deficient character of the aromatics favored the cyclization reaction. Once the cyclic dilactams were made, no problem was encountered to convert it into the corresponding diimidoyl chloride. For the reductive ring closure step, most diimidoyl chlorides succeeded to give the dihydropyrrolo[3,2-*b*]pyrrole core, but with two exceptions: in the case of **7e**, the strong electron-rich character of the final product might easily lead to oxidation, hence no desired product was isolated; in the case of **7m**, an over-reduced product was obtained. With the series of heterocycles bearing the dihydropyrrolo[3,2-*b*]pyrrole core in hand, the effects of substituents and the conjugation length on the energy level of the frontier orbitals were investigated next using UV−vis spectroscopy and cyclic voltammetry. It was found that chlorination and fluorination had quite different effects on the photophysical properties of the heteroacene, and the ring fusing pattern also had a drastic influence on the band gap. Overall, the successful synthesis of a series of heteroacenes bearing a dihydropyrrolo[3,2-*b*]pyrrole core enabled us to investigate their photophysical character systematically and would provide the corresponding candidates for further fabrication of OFET devices. Such work is currently ongoing in our laboratory.

EXPERIMENTAL SECTION

General. All glassware were thoroughly oven-dried. Chemicals and solvents were either purchased from commercial suppliers or purified by standard techniques. Flash chromatography was carried out utilizing silica gel 200−300 mesh. ^{1}H NMR and ^{13}C NMR spectra were recorded with tetramethylsilane (TMS) as an internal standard at 298 K (600 MHz). Cyclic voltammetry was performed using an anhydrous and argon-saturated solution of 0.1 M tetrabutylammonium hexafluorophosphate (n-Bu_4NPF_6) in anhydrous chloroform and a Ag/AgCl electrode as a reference electrode. The potential of Ag/AgCl in THF was determined using ferrocene as an internal standard.

Synthesis of 5g and 5h.

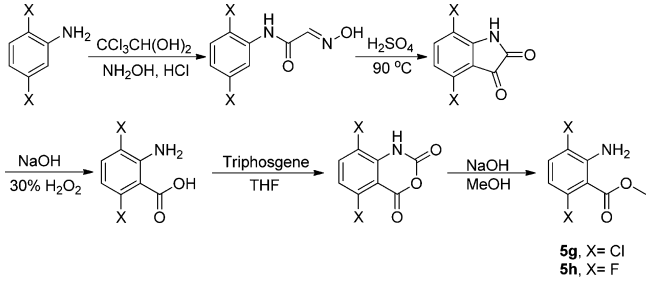

N-(2,5-Dichlorophenyl)-2-(hydroxyimino)acetamide. Anhydrous sodium sulfate (113.6 g, 0.8 mol), hydroxylamine hydrochloride (24.3 g, 0.35 mol), and chloral hydrate (24.8 g, 0.15 mol) were dissolved in water (500 mL). To this solution was added a solution of 2,5-dichloroaminobenzene (16.2 g, 0.1 mol) in water (40 mL), ethanol (70 mL) and concentrated HCl (17 mL). The mixture was heated at 55 °C for 12 h. The crystalline precipitate was filtered, thoroughly washed with water, and dried under vacuum at 50 °C for 24 h to afford 20 g of white solid (87%). ^{1}H NMR (DMSO-d_6, 600 MHz) δ: 12.52 (1H, s), 9.58 (1H, s), 8.08 (1H, d, J = 2.4 Hz), 7.70 (1H, s), 7.60 (1H, d, J = 8.6 Hz), 7.30 (1H, dd, J_1 = 8.6 Hz, J_2 = 2.4 Hz).

4,7-Dichloroindoline-2,3-dione. To 90 mL of concentrated H_2SO_4 (1.84 g/mL) at 50 °C was gradually added with stirring *N*-(2,5-dichlorophenyl)-2-(hydroxyimino)acetamide (19 g, 0.08 mol) so that the temperature of the reaction mixture was within 75−80 °C. Then, the mixture was heated to 80 °C, kept at this temperature for 20 min, cooled to room temperature, poured into a 10−12-fold volume of crushed ice, and allowed to stand for 30 min. Finally, the precipitated product was separated by filtration under vacuum, washed with cold water until the filtrate became neutral, and dried in air to give the product as a red solid (17 g, 98%). ^{1}H NMR (acetone-d_6, 600 MHz) δ: 8.13 (1H, s), 7.51 (1H, d, J = 8.7 Hz), 7.08 (1H, d, J = 8.7 Hz).

2-Amino-3,6-dichlorobenzoic Acid. To the solution of 4,7-dichloroindoline-2,3-dione (17 g, 0.078 mol) in 200 mL of 1 M aqueous NaOH was added dropwise H_2O_2 (22.5 mL, 30%) at rt. The resulting solution was heated to 40 °C for 3 h, then cooled to rt and stirred for another 12 h, acidified by concentrated HCl to get a precipitate, which was then filtered and dried under vacuum at 50 °C for 12 h to give a brown solid product (10.8 g, 67%). ^{1}H NMR (DMSO-d_6, 600 MHz) δ: 13.72 (1H, br), 7.33 (1H, d, J = 8.5 Hz), 6.70 (1H, d, J = 8.5 Hz), 5.76 (1H, br).

5,8-Dichloro-1H-benzo[d][1,3]oxazine-2,4-dione. To a suspension of 2-amino-3,6-dichlorobenzoic acid (10.8 g, 52.4 mmol) in 150 mL of THF was added triphosgene (5.3 g, 17.8 mmol); the reaction mixture was stirred for 12 h, and the resulting precipitate was collected by filtration, which was then washed with 100 mL of ether to give the pure product (11 g, 90%) and used directly for next step.

*Methyl 2-Amino-3,6-dichlorobenzoate (**5g**).* The suspension of 5,8-dichloro-1*H*-benzo[*d*][1,3]oxazine-2,4-dione (11 g, 52.4 mmol) and NaOH (0.56 g, 14 mmol) in 150 mL of absolute MeOH was heated to reflux for 3 h, then MeOH was evaporated to give the crude product, which was then purified by silica column chromatography with petroleum ether/dichloromethane = 3:1 as the eluent (7.0 g, 61%). ^{1}H NMR ($CDCl_3$, 600 MHz) δ: 7.24 (1H, d, J = 8.5 Hz), 6.72 (1H, d, J = 8.5 Hz), 5.38 (2H, br), 4.00 (3H, s). ^{13}C NMR ($CDCl_3$, 150 MHz) δ: 167.2, 145.0, 132.5, 131.8, 119.1, 118.6, 115.5, 52.4.

N-(2,5-Difluorophenyl)-2-(hydroxyimino)acetamide. Anhydrous sodium sulfate (10 g, 70 mmol), hydroxylamine hydrochloride (2.5 g, 35 mmol), and chloral hydrate (2.5 g, 15 mmol) were dissolved in water (45 mL). To this solution was added a solution of 2,5-difluoroaminobenzene (1.3 g, 10 mmol) in water (6 mL) and concentrated HCl (3 mL). The mixture was heated at 100 °C for 1 min. The crystalline precipitate was filtered, thoroughly washed with water, and dried under vacuum at 50 °C for 12 h to afford 1.6 g of white solid (80%). ^{1}H NMR (DMSO-d_6, 600 MHz) δ: 12.40 (1H, s), 9.94 (1H, s), 7.85 (1H, m), 7.80 (1H, s, HC═NOH), 7.35 (1H, m), 7.04 (1H, m). ^{13}C NMR (DMSO-d_6, 150 MHz) δ: 160.91, 158.08 (dd, J_1 = 237.5 Hz, J_2 = 1.9 Hz), 150.30 (dd, J_1 = 240.0 Hz, J_2 = 2.6 Hz), 143.81, 127.11 (dd, J_1 = 13.6 Hz, J_2 = 11.9 Hz), 116.98 (dd, J_1 = 22.3 Hz, J_2 = 9.9 Hz), 112.07 (dd, J_1 = 24.2 Hz, J_2 = 7.8 Hz), 110.85 (d, J = 28.4 Hz).

4,7-Difluoroindoline-2,3-dione. To 5 mL of concentrated H_2SO_4 (1.84 g/mL) at 50 °C was gradually added with stirring *N*-(2,5-difluorophenyl)-2-(hydroxyimino)acetamide (1.5 g, 7.5 mmol) so that the temperature of the reaction mixture was kept within 80−90 °C. Then, the mixture was heated to 90 °C, kept at this temperature for 1 h, cooled to room temperature, poured into a 10−12-fold volume of crushed ice, extracted with ethyl acetate, evaporated to give the crude product which was then purified by column chromatography with petroleum ether/ethyl acetate = 5:1 as eluent to give the pure product (1.05 g, 76%). ^{1}H NMR (acetone-d_6, 600 MHz) δ: 10.68 (1H, br), 7.58 (1H, m), 6.88 (1H, m). ^{13}C NMR (acetone-d_6, 150 MHz) δ: 179.54, 158.88, 155.42 (dd, J_1 = 257.2 Hz, J_2 = 2.1 Hz), 144.80 (dd, J_1 = 239.9 Hz, J_2 = 2.9 Hz), 138.52 (dd, J_1 = 15.4 Hz, J_2 = 6.7 Hz),

dx.doi.org/10.1021/jo501402n | J. Org. Chem. 2014, 79, 11339−11348

127.67 (dd, J_1 = 20.4 Hz, J_2 = 10.2 Hz), 111.28 (dd, J_1 = 22.8 Hz, J_2 = 6.0 Hz), 108.79 (dd, J_1 = 21.0 Hz, J_2 = 3.9 Hz).

2-Amino-3,6-difluorobenzoic Acid. To the solution of 4,7-difluoroindoline-2,3-dione (2.8 g, 1.5 mmol) in 3.3 mL of 1 M of aqueous NaOH was added dropwise H_2O_2 (0.4 mL, 30%) at rt; the resulting solution was heated to 40 °C for 3 h, then cooled to rt and stirred for another 12 h; acidification by concentrated HCl gave a precipitation of the product, which was then filtered and dried under vacuum at 50 °C for 12 h to give the crude product as a brown solid (0.2 g, 80%). ^{1}H NMR (DMSO-d_6, 600 MHz) δ: 13.17 (1H, br), 7.21 (1H, m), 6.59 (2H, br), 6.32 (1H, m). ^{13}C NMR (DMSO-d_6, 150 MHz) δ: 167.39, 158.79 (dd, J_1 = 248.2 Hz, J_2 = 1.9 Hz), 147.32 (dd, J_1 = 233.2 Hz, J_2 = 2.5 Hz), 140.80 (dd, J_1 = 15.8 Hz, J_2 = 5.5 Hz), 118.26 (dd, J_1 = 20.3 Hz, J_2 = 11.8 Hz), 103.22 (dd, J_1 = 16.5 Hz, J_2 = 4.4 Hz), 100.84 (dd, J_1 = 26.4 Hz, J_2 = 7.3 Hz).

5,8-Difluoro-1H-benzo[d][1,3]oxazine-2,4-dione. To a suspension of 2-amino-3,6-difluorobenzoic acid (1.82 g, 10.5 mmol) in 30 mL of THF was added triphosgene (1.07 g, 3.6 mmol); the reaction mixture was stirred for 12 h, and the resulting precipitate was collected by filtration, which was then washed with 100 mL of ether to give the pure product (1.87 g, 98%) and used directly for next step.

*Methyl 2-Amino-3,6-difluorobenzoate (**5h**).* The suspension of 5,8-difluoro-1*H*-benzo[*d*][1,3]oxazine-2,4-dione (2.0 g, 10.4 mmol) and NaOH (0.11 g, 2.6 mmol) in 20 mL of absolute MeOH was heated to reflux for 3 h, then MeOH was evaporated to give the crude product, which was then purified by silica column chromatography with PE/DCM = 1:1 as the eluent to give the product (1.5 g, 76%). ^{1}H NMR ($CDCl_3$, 600 MHz) δ: 7.03 (1H, m), 6.30 (1H, m), 5.82 (2H, br), 3.94 (3H, s). ^{13}C NMR ($CDCl_3$, 150 MHz) δ: 166.79 (dd, J_1 = 4.2 Hz, J_2 = 2.9 Hz), 158.92 (dd, J_1 = 251.5 Hz, J_2 = 2.4 Hz), 147.30 (dd, J_1 = 233.8 Hz, J2=3.0 Hz), 140.27 (dd, J_1 = 15.4 Hz, J_2 = 5.5 Hz), 117.91 (dd, J_1 = 20.6 Hz, J_2 = 11.6 Hz), 102.72 (dd, J_1 = 16.6 Hz, J_2 = 3.9 Hz), 101.70 (dd, J_1 = 26.9 Hz, J_2 = 7.3 Hz), 52.09.

General Procedure for Preparation of the Dilactams. *o*-Aminobenzoate (1.0 equiv) was added dropwise to the suspension of NaH (2.0 equiv, 60%) in anhydrous THF (0.5 mol/L) at 25 °C. The resulting mixture was gradually heated to reflux and stirred for 3 days. The mixture was cooled to rt and then poured slowly into 0.1 M HCl and ice. After the ice had melted, the precipitated product was collected by filtration, washed several times with deionized water, and vacuum-dried at 50 °C to yield the crude product, which was then purified by column chromatography or used directly.

***6a** (75%) and **6b** (75%).* See ref 24.

***6c**[29] (70%).* ^{1}H NMR (600 MHz; DMSO-d_6; Me_4Si) δ 10.67 (1H, s), 8.10 (1H, d, J = 8.5 Hz), 7.86 (1H, d, J = 8.1 Hz), 7.73 (1H, d, J = 8.5 Hz), 7.67−7.66 (1H, m), 7.58−7.57 (1H, m), 7.33 (1H, d, J = 8.5 Hz). ^{13}C NMR (150 MHz; DMSO-d_6; Me_4Si) δ 170.2, 134.1, 131.5, 130.7, 128.9, 128.5, 128.2, 128.0, 127.9, 124.3, 123.8. HRMS (ESI-TOF) calcd for $C_{22}H_{14}N_2O_2Na$ $[M + Na]^+$, 361.0948, found 361.0947. mp: > 300 °C. IR (KBr, cm^{-1}): 3440, 3351, 3170, 3058, 1651, 1393, 824, 754.

***6e** (75%).* ^{1}H NMR (600 MHz; DMSO-d_6; Me_4Si) δ 9.78 (1H, s), 6.81 (1H, s), 6.61 (1H, s), 3.73 (3H, s), 3.72 (3H, s). ^{13}C NMR (150 MHz; DMSO-d_6; Me_4Si) δ 169.7, 150.3, 147.9, 129.0, 125.7, 111.0, 109.6, 56.2, 56.1. HRMS (ESI-TOF) calcd for $C_{18}H_{19}N_2O_6$ $[M + H]^+$, 359.1243, found 359.1234. mp: > 300 °C. IR (KBr, cm^{-1}): 3298, 2923, 2853, 1672, 1340, 1515, 1465, 1399, 1266, 1221, 1072, 984, 866, 777.

***6f** (95%).* ^{1}H NMR (600 MHz; DMSO-d_6; Me_4Si) δ 10.37 (1H, s), 7.58 (1H, dd, J_1 = 8.5 Hz, J_2 = 2.4 Hz), 7.51 (1H, d, J = 2.4 Hz), 7.10 (1H, d, J = 8.5 Hz). ^{13}C NMR (150 MHz; DMSO-d_6; Me_4Si) δ 167.8, 135.6, 134.3, 134.0, 131.1, 128.5, 120.4. HRMS (ESI-TOF) calcd for $C_{14}H_9Br_2N_2O_2$ $[M + H]^+$, 396.9010, found 396.8998. mp: > 300 °C. IR (KBr, cm^{-1}): 3166, 3049, 2872, 1655, 1485, 1423, 1355, 1260, 1104, 829, 700.

***6g** (75%).* ^{1}H NMR (600 MHz; DMSO-d_6; Me_4Si) δ 10.99 (1H, s), 7.58 (1H, d, J = 8.4 Hz), 7.44 (1H, d, J = 8.4 Hz). ^{13}C NMR (150 MHz; DMSO-d_6; Me_4Si) δ 164.9, 134.8, 133.8, 131.9, 130.7, 130.0, 128.9. HRMS (ESI-TOF) calcd for $C_{14}H_7N_2O_2Cl_4$ $[M + H]^+$, 374.9256, found 374.9259. mp: > 300 °C. IR (KBr, cm^{-1}): 3198, 2876, 1699, 1671, 1579, 1469, 1416, 1366, 1180, 1131, 966, 823, 746.

***6h** (60%).* ^{1}H NMR (600 MHz; DMSO-d_6; Me_4Si) δ 10.88 (1H, s), 7.46−7.42 (1H, m), 7.32−7.28 (1H, m). ^{13}C NMR (150 MHz; DMSO-d_6; Me_4Si) δ 163.1 (d, J = 1.5 Hz), 154.3 (dd, J_1 = 230.8 Hz, J_2 = 2.5 Hz), 152.6 (dd, J_1 = 230.8 Hz, J_2 = 2.5 Hz), 124.0 (dd, J_1 = 17.1 Hz, J_2 = 6.0 Hz), 153.3 (d, J = 20.7 Hz), 118.9 (dd, J_1 = 22.6 Hz, J_2 = 9.7 Hz), 117.3 (dd, J_1 = 23.7 Hz, J_2 = 8.0 Hz). HRMS (ESI-TOF) calcd for $C_{14}H_7N_2O_2F_4$ $[M + H]^+$, 311.0438, found 311.0442. mp: > 300 °C. IR (KBr, cm^{-1}): 3192, 2932, 1687, 1625, 1499, 1450, 1376, 1246, 1136, 1051, 928, 832, 720.

***6i** (26%).* ^{1}H NMR (600 MHz; DMSO-d_6; Me_4Si) δ 10.39 (1H, s), 7.49−7.46 (1H, m), 7.26−7.23 (1H, m). ^{13}C NMR (150 MHz; DMSO-d_6; Me_4Si) δ 167.3, 150.2 (dd, J_1 = 198 Hz, J_2 = 13.3 Hz), 148.5 (dd, J_1 = 198 Hz, J_2 = 13.3 Hz), 132.2 (dd, J_1 = 8.6 Hz, J_2 = 3.1 Hz), 130.8 (m), 116.0 (d, J = 18.3 Hz), 117.5 (d, J = 19.6 Hz). HRMS (ESI-TOF) calcd for $C_{14}H_7N_2O_2F_4$ $[M + H]^+$, 311.0438, found 311.0442. mp: > 300 °C. IR (KBr, cm^{-1}): 3189, 3071, 2954, 1686, 1667, 1518, 1426, 1352, 1282, 1045, 887, 804, 777.

***6k** (26%).* See ref 29.

***6l** (90%).* ^{1}H NMR (600 MHz; DMSO-d_6; Me_4Si) δ 11.30 (1H, s), 8.60 (1H, s), 7.98 (1H, d, J = 8.2 Hz), 7.90 (1H, d, J = 8.6 Hz), 7.80−7.79 (1H, t, J = 6.0 Hz), 7.59−7.58 (1H, t, J = 6.0 Hz). ^{13}C NMR (150 MHz; DMSO-d_6; Me_4Si) δ 168.2, 147.2, 146.5, 139.6, 132.3, 128.8, 128.4, 127.8*2, 126.6. HRMS (ESI-TOF) calcd for $C_{20}H_{13}N_4O_2$ $[M + H]^+$, 341.1033, found 341.1036. mp: > 300 °C. IR (KBr, cm^{-1}): 3175, 3065, 2918, 1670, 1621, 1594, 1494, 1445, 1418, 1398, 1327, 1301, 1135, 967, 925, 783, 749.

***6m** (96%).* ^{1}H NMR (600 MHz; DMSO-d_6; Me_4Si) δ 11.30 (1H, s), 8.60 (1H, s), 7.98 (1H, d, J = 8.2 Hz), 7.90 (1H, d, J = 8.6 Hz), 7.80−7.79 (1H, t, J = 6.0 Hz), 7.59−7.58 (1H, t, J = 6.0 Hz). ^{13}C NMR (150 MHz; DMSO-d_6; Me_4Si) δ 167.7, 152.9, 146.4, 133.3, 131.1, 129.1, 128.8, 128.4, 128.0*2. HRMS (ESI-TOF) calcd for $C_{20}H_{13}N_4O_2$ $[M + H]^+$, 341.1033, found 341.1036. mp: > 300 °C. IR (KBr, cm^{-1}): 3064, 3009, 2099, 1683, 1598, 1500, 1475, 1393, 1371, 1331, 1202, 1136, 1078, 770, 744.

General Procedure for Preparation of the Heteroacenes. *Preparation of Imidoyl Chlorides.* Finely powdered diamide (1.0 equiv) and phosphorus pentachloride (2.0−4.0 equiv) were boiled together in chloroform for 4 h, then cooled to ambient temperature and evaporated to give the crude product which was used directly in next step unless otherwise mentioned.

Preparation of the Heteroacenes. To the solution (0.04 mol/L) of imidoyl chloride in anhydrous THF was added activated zinc (12.0 equiv) in one portion, then TFA(24.0 equiv) was added dropwise at rt. The resulting suspension was stirred for 12 h at that temperature, then saturated aqueous NH_4Cl was added to quench the reaction. The mixture was extracted with ethyl acetate and dried over anhydrous Na_2SO_4. Removal of the solvent under under reduced pressure afforded the crude product, which was then purified by column chromatography.

***7e** (45%).* The crude product was purified by column chromatography with dichloromethane/petroleum ether = 5:1 as eluent. ^{1}H NMR (600 MHz; $CDCl_3$; Me_4Si) δ 6.74 (1H, s), 6.48 (1H, s), 3.88 (3H, s), 3.87 (3H, s). ^{13}C NMR (150 MHz; $CDCl_3$; Me_4Si) δ 156.1, 151.8, 146.6, 140.0, 117.5, 109.2, 105.3, 56.2, 56.1. HRMS (ESI-FTMS) calcd for $C_{18}H_{16}N_2O_4Cl_2$ $[M]^+$, 395.0560, found 395.0565. mp: 160 °C (dec.). IR (KBr, cm^{-1}): 2956, 2926, 2855, 1732, 1653, 1603, 1509, 1462, 1420, 1365, 1263, 1221, 1169, 1094, 928, 860,747.

***7l** (45%).* The crude product was purified by column chromatography with dichloromethane/petroleum ether = 5:1 as eluent. ^{1}H NMR (600 MHz; $CDCl_3$; Me_4Si) δ 8.32 (1H, s), 7.93 (1H, d, J = 8.6 Hz), 7.79 (1H, d, J = 8.3 Hz), 7.73 (1H, t,J = 7.8 Hz), 7.51 (1H, t, J = 7.8 Hz). ^{13}C NMR (150 MHz; $CDCl_3$; Me_4Si) δ 157.4, 153.2, 148.1,137.8, 132.5, 128.7, 128.3, 127.3, 124.8, 122.1. HRMS (ESI-FTMS) calcd for $C_{20}H_{11}N_4Cl_2$ $[M + H]^+$, 377.0355, found 377.0361. mp: > 300 °C. IR (KBr, cm^{-1}): 2923, 1663, 1617, 1588, 1488, 1409, 1249, 1175, 1120, 912, 783.

***7m** (50%).* The crude product was purified by column chromatography with dichloromethane/petroleum ether = 5:1 as eluent. ^{1}H NMR (600 MHz; $CDCl_3$; Me_4Si) δ 8.04 (1H, d, J = 8.4 Hz), 7.89 (1H, s), 7.76 (1H, d, J = 8.4 Hz), 7.68 (1H, t, J = 7.0 Hz),

7.57 (1H, t, J = 7.0 Hz). ^{13}C NMR (150 MHz; $CDCl_3$; Me_4Si) δ 156.7, 145.5, 143.8, 137.7, 130.1, 129.5, 129.0, 128.7, 128.2, 127.6. HRMS (ESI-FTMS) calcd for $C_{20}H_{11}N_4Cl_2$ $[M + H]^+$, 377.0355, found 377.0361. mp: > 300 °C. IR (KBr, cm^{-1}): 2954, 2923, 2852, 1731, 1654, 1486, 1453, 1373, 1258, 1189, 1117, 1014, 939, 819, 753.

***1a** (70%) and **1b** (50%).* See ref 24.

***1c** (30%).* ^{1}H NMR (600 MHz; DMSO-d_6; Me_4Si) δ 10.67 (1H, s), 8.10 (1H, d, J = 8.5 Hz), 7.86 (1H, d, J = 8.1 Hz), 7.73 (1H, d, J = 8.5 Hz), 7.67−7.66 (1H, m), 7.58−7.57 (1H, m), 7.33 (1H, d, J = 8.5 Hz). ^{13}C NMR (150 MHz; DMSO-d_6; Me_4Si) δ 170.2, 134.1, 131.5, 130.7, 128.9, 128.5, 128.2, 128.0, 127.9, 124.3, 123.8. HRMS (ESI-TOF) calcd for $C_{22}H_{14}N_2O_2Na$ $[M + Na]^+$, 361.0948, found 361.0947. mp: > 300 °C. IR (KBr, cm^{-1}): 3440, 3351, 3170, 3058, 1651, 1393, 824, 754.

***1f** (53%).* ^{1}H NMR (600 MHz; $CDCl_3$; Me_4Si) δ 11.31 (2H, s, NH), 7.89(2H, d, J = 1.8 Hz, Ar), 7.50(2H, d, J = 8.6 Hz, Ar), 7.30 (2H, dd, J_1 = 8.6 Hz, J_2 = 1.8 Hz, Ar). ^{13}C NMR (150 MHz; $CDCl_3$; Me_4Si) δ 139.5, 125.9, 124.8, 120.4, 116.2, 114.7, 110.6. HRMS (ESI-TOF) calcd for $C_{14}H_8Br_2N_2$ $[M + Na]^+$, 385.2929, found 385.2929. mp: > 300 °C. IR (KBr, cm^{-1}): 3400, 1664, 1560, 1454, 1356, 1308, 1223, 1159, 1046, 949, 862, 798, 687.

***1g** (35%).* ^{1}H NMR (600 MHz; DMSO-d_6; Me_4Si) δ 11.78 (1H, s), 7.36 (1H, d, J = 8.4 Hz), 7.22 (1H, d, J = 8.4 Hz). ^{13}C NMR (150 MHz; DMSO-d_6; Me_4Si) δ 138.4, 125.9, 123.7, 122.6, 119.7, 116.0, 115.4. HRMS (ESI-FTMS) calcd for $C_{14}H_6N_2Cl_4$ $[M]^+$, 341.9280, found 341.9283. mp: 277.7−280.9 °C. IR (KBr, cm^{-1}): 3455, 1813, 1646, 1517, 1441, 1372, 1343, 1300, 1202, 1150, 989, 932, 817, 784.

***1h** (37%).* ^{1}H NMR (600 MHz; DMSO-d_6; Me_4Si) δ 12.29 (1H, s), 7.10−7.18 (1H, m), 6.90−6.87 (1H, m). ^{13}C NMR (150 MHz; DMSO-d_6; Me_4Si) δ 151.5 (d, J = 240 Hz), 146.2 (d, J = 240 Hz), 130.5 (dd, J_1 = 17 Hz, J_2 = 11 Hz), 123.7 (d, J = 2.8 Hz), 107.7 (dd, J_1 = 19.6 Hz, J_2 = 8.6 Hz), 106.5 (dd, J_1 = 25 Hz, J_2 = 7 Hz), 103.2 (dd, J_1 = 21.2 Hz, J_2 = 7.4 Hz). HRMS (ESI-FTMS) calcd for $C_{14}H_6F_4N_2$ $[M]^+$, 278.0462, found 278.0463. mp: > 300 °C. IR (KBr, cm^{-1}): 3471, 1637, 1535, 1459, 1400, 1360, 1335, 1228, 1205, 1139, 1057, 1017, 783, 707.

***1i** (37%).* ^{1}H NMR (600 MHz; DMSO-d_6; Me_4Si) δ 11.22 (1H, s), 7.68−7.64 (1H, m), 7.57−7.54 (1H, m). ^{13}C NMR (150 MHz; DMSO-d_6; Me_4Si) δ 147.2 (dd, J_1 = 238 Hz, J_2 = 15.6 Hz), 144.8 (dd, J_1 = 234 Hz, J_2 = 14.7 Hz), 135.9 (d, J = 10.7 Hz), 126.9, 110.2 (d, J =8.9 Hz), 104.7 (d, J = 19.9 Hz), 100.9 (d, J = 21.5 Hz). HRMS (ESI-FTMS) calcd for $C_{14}H_6F_4N_2$ $[M]^+$, 278.0462, found 278.0463. mp: 297.2 °C (dec.). IR (KBr, cm^{-1}): 3484, 3446, 3396, 1683, 1588, 1477, 1419, 1315, 1267, 1208, 1196, 1143, 1100, 904, 854, 803, 725.

***1k** (37%).* ^{1}H NMR (600 MHz; TFA-d; Me_4Si) δ 9.31 (1H, d, J = 8.4 Hz), 8.71 (1H, d, J = 6 Hz), 7.89 (1H, dd, J_1 = 8.4 Hz, J_2 = 6 Hz). ^{13}C NMR (150 MHz; TFA-d; Me_4Si) δ 141.5, 137.6, 133.9, 123.6, 116.1, 114.0. HRMS (ESI-FTMS) calcd for $C_{12}H_9N_4$ $[M + H]^+$, 209.0822, found 209.0821. mp: > 300 °C. IR (KBr, cm^{-1}): 3279, 2936, 1637, 1573, 1455, 1379, 1287, 1240, 1146, 1050, 934, 780.

***1l** (30%).* ^{1}H NMR (600 MHz; TFA-d; Me_4Si) δ 9.75 (1H, s), 8.45 (1H, d, J = 8.3 Hz), 8.31 (1H, d, J = 8.3 Hz), 8.23 (1H, t, J = 7.5 Hz), 7.97 (1H, t, J = 7.5 Hz). ^{13}C NMR (150 MHz; TFA-d; Me_4Si) δ 144.0, 138.0, 135.1, 134.3, 130.0 127.2, 124.5, 123.1, 118.2, 112.9. HRMS (ESI-FTMS) calcd for $C_{20}H_{13}N_4$ $[M + H]^+$, 309.1135, found 309.1129. mp: > 300 °C. IR (KBr, cm^{-1}): 3401, 3099, 3045, 1612, 1574, 1489, 1449, 1398, 1274, 1224, 1190, 1138, 1095, 946, 894, 748.

General Procedure for Preparation of the Alkylated Heteroacenes. A freshly prepared 50% aqueous NaOH solution (50.0 equiv) was added to a well-stirred mixture of heteroacene (1.0 equiv), benzyltriethylammonium chloride (0.2 equiv), 1-bromooctane (5.0 equiv), and DMSO (0.025 mol/L) in a flask under an argon atmosphere. The mixture was stirred at room temperature for 12 h. Subsequently, the reaction mixture was poured into 20 mL of water, then extracted with dichloromethane; the organic layer was separated, dried over $MgSO_4$, filtered, and the solvent removed using a rotary evaporator, and the resulting crude product was washed with ether to give the pure product.

***8a** (85%).* ^{1}H NMR (600 MHz; acetone-d_6; Me_4Si) δ 7.92 (1H, d, J = 7.8 Hz); 7.59 (1H, d, J = 8.4 Hz), 7.26 (1H, t, J = 7.5 Hz), 7.15 (1H, t, J =7.5 Hz), 4.5 (2H, t, J = 7.0 Hz), 1.98 (2H, m), 1.41 (10H, m), 0.89 (3H, t, J = 7.0 Hz). ^{13}C NMR (150 MHz; acetone-d_6; Me_4Si) δ 140.7, 125.7, 121.5, 118.0, 117.7, 114.6, 110.0, 44.7, 31.6, 30.2, 26.8, 22.3, 13.4. HRMS (ESI-TOF) calcd for $C_{30}H_{42}N_2Na$ $[M + Na]^+$, 453.3240, found 453.3230. mp: 74.1−75.2 °C. IR (KBr, cm^{-1}): 3061, 2956, 2927, 2851, 1494, 1474, 1414, 1343, 1269, 1185, 1126, 1019, 916, 836, 735.

***8b** (86%).* ^{1}H NMR (600 MHz; $CDCl_3$; Me_4Si) δ 8.33 (2H, s), 8.04 (1H, d, J = 8.15 Hz), 8.00 (1H, d, J = 8.15 Hz), 7.43−7.38 (2H, m), 4.67 (2H, t, J = 7.2 Hz), 2.08 (2H, m), 1.50−1.23 (10H, m), 0.83 (3H, t, J = 7 Hz). ^{13}C NMR (150 MHz; $CDCl_3$; Me_4Si) δ 141.8, 130.1, 128.1, 128.0, 127.6, 127.4, 124.0, 122.5, 117.1, 115.4, 105.0, 45.7, 31.8, 30.2, 29.5, 29.2, 27.3, 22.6, 14.1. HRMS (ESI-TOF) calcd for $C_{38}H_{47}N_2$ $[M + H]^+$, 531.3734, found 531.3703. mp: 170.0−171.4 °C. IR (KBr, cm^{-1}): 3335, 2921, 2851, 1732, 1671, 1476, 1371, 1202, 849, 738.

***8c** (80%).* ^{1}H NMR (600 MHz; acetone-d_6; Me_4Si) δ 8.63 (1H, d, J = 8.0 Hz), 8.22 (1H, d, J = 8.4 Hz), 8.06 (1H, d, J = 7.4 Hz), 7.69−7.65 (2H, m), 7.50 (1H, m), 5.18−5.17(2H, m), 2.19−2.18 (2H, m), 1.58−1.24 (10H, m), 0.83−0.80 (3H, m). ^{13}C NMR (150 MHz; acetone-d_6; Me_4Si) δ 133.6, 131.4, 129.3, 126.9, 125.5, 123.6, 123.3, 121.2, 120.1, 117.7, 111.5, 48.6, 31.6, 30.4, 26.5, 22.4, 13.4. mp: 141.3−142.1 °C. IR (KBr, cm^{-1}): 3045, 2950, 2923, 2852, 1614, 1488, 1465, 1432, 1379, 1274, 1253, 1162, 1126, 1050, 849, 797, 732.

***8g** (85%).* ^{1}H NMR (600 MHz; $CDCl_3$; Me_4Si) δ 7.20 (1H, s), 7.12 (1H, d, J = 8.4 Hz), 5.26 (2H, d, J = 7.2 Hz), 71.73−1.72 (2H, m), 1.23−1.17 (10H, m), 0.84 (3H, t, J = 7.2 Hz). ^{13}C NMR (150 MHz; $CDCl_3$; Me_4Si) δ 138.6, 128.4, 125.6, 122.5, 121.4, 117.2, 116.5, 48.2, 31.7, 31.1, 29.2, 29.1, 26.2, 22.6, 14.1. HRMS (ESI-TOF) calcd for $C_{30}H_{39}Cl_4N_2$ $[M + H]^+$, 567.1862, found 567.1848. mp: 106.9−107.1 °C. IR (KBr, cm^{-1}): 2951, 2919, 2852, 1646, 1476, 1426, 1374, 1204, 1152, 1040, 959, 791.

***8h** (85%).* ^{1}H NMR (600 MHz; $CDCl_3$; Me_4Si) δ 6.94−6.90 (1H, m), 6.77−6.73 (1H, m), 4.70 (2H, d, J = 7.2 Hz), 1.90 (2H, t, J = 7.2 Hz), 1.37−1.24 (10H, m), 0.88 (3H, t, J = 7.2 Hz). ^{13}C NMR (150 MHz; $CDCl_3$; Me_4Si) δ 151.5 (d, J = 240 Hz), 145.5 (d, J = 240 Hz), 129.6 (d, J = 11 Hz), 125.2, 108.0 (dd, J_1 = 22 Hz, J_2 = 9.2 Hz), 106.4 (dd, J_1 = 24 Hz, J_2 = 6.5 Hz), 102.9 (dd, J_1 = 24 Hz, J_2 = 7.8 Hz). HRMS (ESI-TOF) calcd for $C_{30}H_{39}F_4N_2$ $[M + H]^+$, 503.3044, found 503.3055. mp: 69.7−70.4 °C. IR (KBr, cm^{-1}): 2956, 2929, 2854, 1522, 1484, 1453, 1375, 1227, 1144, 1117, 1054, 781.

***8l** (75%).* ^{1}H NMR (600 MHz; $CDCl_3$; Me_4Si) δ 8.57 (s, 1H), 8.15 (d, J = 8.4 Hz, 1H), 8.03 (d, J = 8.2 Hz, 1H), 7.70 (t, J = 7.5 Hz, 1H), 7.47 (t, J = 7.5 Hz, 1H), 4.84 (t, J = 7.2 Hz, 2H), 2.12−2.10 (m, 2H), 1.48−1.42 (m, 10H), 0.82 (t, J = 6.5 Hz, 3H). ^{13}C NMR (150 MHz; $CDCl_3$; Me_4Si) δ 151.4, 144.9, 128.3, 128.1, 128.0, 124.5, 124.4, 123.8, 122.9, 110.5, 43.7, 31.8, 30.2, 29.3, 29.2, 27.0, 22.6, 14.1. HRMS (ESI-TOF) calcd for $C_{36}H_{45}N_4$ $[M + H]^+$, 533.3639, found 533.3637. mp: 211.5−213.6 °C. IR (KBr, cm^{-1}): 3048, 2921, 2851, 1604, 1569, 1506, 1481, 1380, 1259, 1205, 1125, 1011, 879, 750.

■ ASSOCIATED CONTENT

Ⓢ Supporting Information

Calculated results and characterization data of all new compounds. This material is available free of charge via the Internet at http://pubs.acs.org.

■ AUTHOR INFORMATION

Corresponding Author

*E-mail: wanxb@qibebt.ac.cn. Phone: 86-532-80662740.

Notes

The authors declare no competing financial interest.

■ ACKNOWLEDGMENTS

This work was supported by the "100 Talents" program from the Chinese Academy of Sciences and National Science Foundation of China (21174157, 21103213, 91233106). We

also thank Prof. Pratap Bahadur from VNSG University Surat India for manuscript proof-reading.

REFERENCES

(1) Wang, C.; Dong, H.; Hu, W.; Liu, Y.; Zhu, D. *Chem. Rev.* **2012**, *112*, 2208.
(2) Mei, J.; Diao, Y.; Appleton, A. L.; Fang, L.; Bao, Z. *J. Am. Chem. Soc.* **2013**, *135*, 6724.
(3) Takimiya, K.; Kunugi, Y.; Konda, Y.; Ebata, H.; Toyoshima, Y.; Otsubo, T. *J. Am. Chem. Soc.* **2006**, *128*, 3044.
(4) Ebata, H.; Izawa, T.; Miyazaki, E.; Takimiya, K.; Ikeda, M.; Kuwabara, H.; Yui, T. *J. Am. Chem. Soc.* **2007**, *129*, 15732.
(5) Yamamoto, T.; Takimiya, K. *J. Am. Chem. Soc.* **2007**, *129*, 2224.
(6) Shinamura, S.; Miyazaki, E.; Takimiya, K. *J. Org. Chem.* **2010**, *75*, 1228.
(7) Nakano, M.; Mori, H.; Shinamura, S.; Takimiya, K. *Chem. Mater.* **2011**, *24*, 190.
(8) Niimi, K.; Kang, M. J.; Miyazaki, E.; Osaka, I.; Takimiya, K. *Org. Lett.* **2011**, *13*, 3430.
(9) Niimi, K.; Shinamura, S.; Osaka, I.; Miyazaki, E.; Takimiya, K. *J. Am. Chem. Soc.* **2011**, *133*, 8732.
(10) Shinamura, S.; Osaka, I.; Miyazaki, E.; Nakao, A.; Yamagishi, M.; Takeya, J.; Takimiya, K. *J. Am. Chem. Soc.* **2011**, *133*, 5024.
(11) Takimiya, K.; Shinamura, S.; Osaka, I.; Miyazaki, E. *Adv. Mater.* **2011**, *23*, 4347.
(12) Yamamoto, T.; Nishimura, T.; Mori, T.; Miyazaki, E.; Osaka, I.; Takimiya, K. *Org. Lett.* **2012**, *14*, 4914.
(13) Kang, M. J.; Miyazaki, E.; Osaka, I.; Takimiya, K.; Nakao, A. *ACS Appl. Mater. Interfaces* **2013**, *5*, 2331.
(14) Mori, T.; Nishimura, T.; Yamamoto, T.; Doi, I.; Miyazaki, E.; Osaka, I.; Takimiya, K. *J. Am. Chem. Soc.* **2013**, *135*, 13900.
(15) Minemawari, H.; Yamada, T.; Matsui, H.; Tsutsumi, J. y.; Haas, S.; Chiba, R.; Kumai, R.; Hasegawa, T. *Nature* **2011**, *475*, 364.
(16) Saito, M.; Osaka, I.; Miyazaki, E.; Takimiya, K.; Kuwabara, H.; Ikeda, M. *Tetrahedron Lett.* **2011**, *52*, 285.
(17) Tanaka, S.; Kumagai, T.; Mukai, T.; Kobayashi, T. *Bull. Chem. Soc. Jpn.* **1987**, *60*, 1981.
(18) Samsoniya, S. A.; Trapaidze, M. V. *Russ. Chem. Rev.* **2007**, *76*, 313.
(19) Ruggli, P.; Zaeslin, H. *Helv. Chim. Acta* **1935**, *18*, 845.
(20) Murray, M. M.; Kaszynski, P.; Kaisaki, D. A.; Chang, W.; Dougherty, D. A. *J. Am. Chem. Soc.* **1994**, *116*, 8152.
(21) Jin, Y.; Kim, K.; Song, S.; Kim, J.; Kim, J.; Park, S. H.; Lee, K.; Suh, H. *Bull. Korean Chem. Soc.* **2006**, *27*, 1043.
(22) Owczarczyk, Z. R.; Braunecker, W. A.; Garcia, A.; Larsen, R.; Nardes, A. M.; Kopidakis, N.; Ginley, D. S.; Olson, D. C. *Macromolecules* **2013**, *46*, 1350.
(23) Kaszynski, P.; Dougherty, D. A. *J. Org. Chem.* **1993**, *58*, 5209.
(24) Grinyov, A. N.; Ryabova, S. Y. *Khim. Geterotsikl. Soedin.* **1982**, 199.
(25) Jackson, A. H.; Johnston, D. N.; Shannon, P. V. R. *J. Chem. Soc., Chem. Commun.* **1975**, 911.
(26) Janiga, A.; Bednarska, D.; Thorsted, B.; Brewer, J.; Gryko, D. T. *Org. Biomol. Chem.* **2014**, *12*, 2874.
(27) Krzeszewski, M.; Thorsted, B.; Brewer, J.; Gryko, D. T. *J. Org. Chem.* **2014**, *79*, 3119.
(28) Qiu, L.; Yu, C. M.; Zhao, N.; Chen, W. C.; Guo, Y. L.; Wan, X. B.; Yang, R. Q.; Liu, Y. Q. *Chem. Commun.* **2012**, *48*, 12225.
(29) Qiu, L.; Zhuang, X.; Zhao, N.; Wang, X.; An, Z.; Lan, Z.; Wan, X. *Chem. Commun.* **2014**, *50*, 3324.
(30) Cooper, F. C.; Partridge, M. W. *J. Chem. Soc.* **1955**, 991.
(31) Hoorfar, A.; Ollis, W. D.; Price, J. A.; Stephanatou, J. S.; Stoddart, J. F. *J. Chem. Soc., Perkin Trans. 1* **1982**, 1649.
(32) Gordon-Wylie, S. W.; Teplin, E.; Morris, J. C.; Trombley, M. I.; McCarthy, S. M.; Cleaver, W. M.; Clark, G. R. *Cryst. Growth Des.* **2004**, *4*, 789.
(33) Pardo, C.; Pirat, C.; Elguero, J. *J. Heterocycl. Chem.* **2007**, *44*, 1303.
(34) Tang, M. L.; Oh, J. H.; Reichardt, A. D.; Bao, Z. *J. Am. Chem. Soc.* **2009**, *131*, 3733.
(35) Liang, Z.; Tang, Q.; Xu, J.; Miao, Q. *Adv. Mater.* **2011**, *23*, 1535.
(36) Swartz, C. R.; Parkin, S. R.; Bullock, J. E.; Anthony, J. E.; Mayer, A. C.; Malliaras, G. G. *Org. Lett.* **2005**, *7*, 3163.